

## Molecular Dynamics Study of the Inclusion of Cholesterol into Cyclodextrins

Yanmin Yu,<sup>†</sup> Christophe Chipot,<sup>‡</sup> Wensheng Cai,<sup>\*,†,§</sup> and Xueguang Shao<sup>§</sup>

Department of Chemistry, University of Science and Technology of China, Hefei, Anhui, 230026, P R China, Equipe de dynamique des assemblages membranaires, UMR CNRS/UHP 7565, Université Henri Poincaré, BP 239, 54506 Vandœuvre-lès-Nancy Cedex, France, and Department of Chemistry, Nankai University, Tianjin, 300071, P R China

Received: November 21, 2005; In Final Form: January 31, 2006

The interaction of three cyclodextrins (CDs), viz.  $\beta$ -CD, heptakis (2,6-di-O-methyl)- $\beta$ -CD (DM- $\beta$ -CD), and 2-hydroxypropyl- $\beta$ -CD (HP- $\beta$ -CD), with cholesterol was investigated using molecular dynamics (MD) simulations. The free energy along the reaction pathway delineating the inclusion of cholesterol into each CD was computed using the adaptive biasing force method. The association constant and the corresponding association free energy were derived by integrating the potential of mean force (PMF) over a representative ordering parameter. The results show that the free energy profiles possess two local minima corresponding to roughly equally probable binding modes. Among the three CDs, DM- $\beta$ -CD exhibits the highest propensity to associate with cholesterol. Ranking for binding cholesterol, viz. DM- $\beta$ -CD > HP- $\beta$ -CD >  $\beta$ -CD, agrees nicely with experiment. Partitioning of the PMF into free energy components illuminates that entering of cholesterol into the CD cavity is driven mainly by electrostatic interactions, whereas deeper inclusion results from van der Waals forces and solvation effects. Additional MD simulations were performed to investigate the structural stability of the host–guest complexes near the free energy minima. The present results demonstrate that association of cholesterol and CDs follows two possible binding modes. Although the latter are thermodynamically favorable for all CDs, one of the two inclusion complexes appears to be preferred kinetically in the case of DM- $\beta$ -CD.

## 1. Introduction

Cholesterol is an important structural component of the mammalian cellular plasma membrane. It is involved in regulating membrane permeability and fluidity. Cholesterol is also a primary constituent of lipid–protein assemblies in the plasma membrane, which are involved in cellular signal transduction, immune response, cell infection, and cell surface polarity.<sup>1</sup> Cholesterol consists of a planar tetracyclic ring system with a hydroxyl group and a short eight-carbon atom chain. It is largely hydrophobic. Alternatively, cyclodextrins (CDs) are cyclic oligosaccharides formed by the bacterial degradation of starch and typically contain six (i.e.,  $\alpha$ -CD), seven (i.e.,  $\beta$ -CD), or eight (i.e.,  $\gamma$ -CD) glucose repetitive units linked together by 1–4 glycosidic bonds.<sup>2</sup> CD molecules have a hydrophilic outer surface and a hydrophobic inner core, conducive to the formation of inclusion complexes through the binding of small molecules into their core.<sup>3–5</sup>

In recent years, CDs have been used as tools to manipulate the lipid composition of biological and model membranes.<sup>6–12</sup> Among the three families of CDs,  $\beta$ -CDs are known to be very efficient sterol-acceptor molecules, apparently because their inner hydrophobic cavity matches the size of the sterol molecule. Compared to the simple  $\beta$ -CD,  $\beta$ -CD derivatives have been shown to improve greatly the solvation of sterols in aqueous

solutions.<sup>13–17</sup> The interaction of CDs with cholesterol has been investigated in detail, at both the theoretical and experimental levels, in monolayer and bilayer membrane model systems as well as in living cells.<sup>18–30</sup> Yet, despite the demonstrated effectiveness of CDs in biomedical applications, relatively little is known about the free energy change along the reaction pathway for cholesterol inclusion into CDs or the detailed mechanism governing the latter. In this paper, the interaction of CDs with cholesterol is examined in aqueous solution. The results reported here constitute the first step of a broader study, which will eventually include a lipid bilayer. It is, however, crucial to understand first the basic underlying mechanisms that drive cholesterol recognition and association with CDs.

Here, variation of the free energy along a chosen ordering parameter delineating host–guest inclusion was examined using molecular dynamics (MD) simulations and the adaptive biasing force (ABF)<sup>31–34</sup> method for the complex of cholesterol with  $\beta$ -CD, 2-hydroxypropyl- $\beta$ -CD (HP- $\beta$ -CD), and heptakis (2,6-di-O-methyl)- $\beta$ -CD (DM- $\beta$ -CD). The association constant and the corresponding association free energy were obtained by integrating the potential of mean force (PMF) over the interval characterizing molecular association. It will be shown that for the three CDs, the order of efficiency in accepting cholesterol is DM- $\beta$ -CD > HP- $\beta$ -CD >  $\beta$ -CD, in nice agreement with experiment. Partitioning of the PMF into free energy components helps us understand how cholesterol binds to the CD cavity. The stationary points found on the free energy landscape were further examined by means of additional MD simulations. Thorough analysis of the MD trajectories sheds new light on the noteworthy stability of the inclusion complexes.

\* Corresponding author address: Department of Chemistry, University of Science and Technology of China, Hefei, Anhui, 230026, P R China. Tel: +86-551-3606160. Fax: +86-551-3601592. E-mail: wscail@ustc.edu.cn.

<sup>†</sup> University of Science and Technology of China.

<sup>‡</sup> Université Henri Poincaré.

<sup>§</sup> Nankai University.

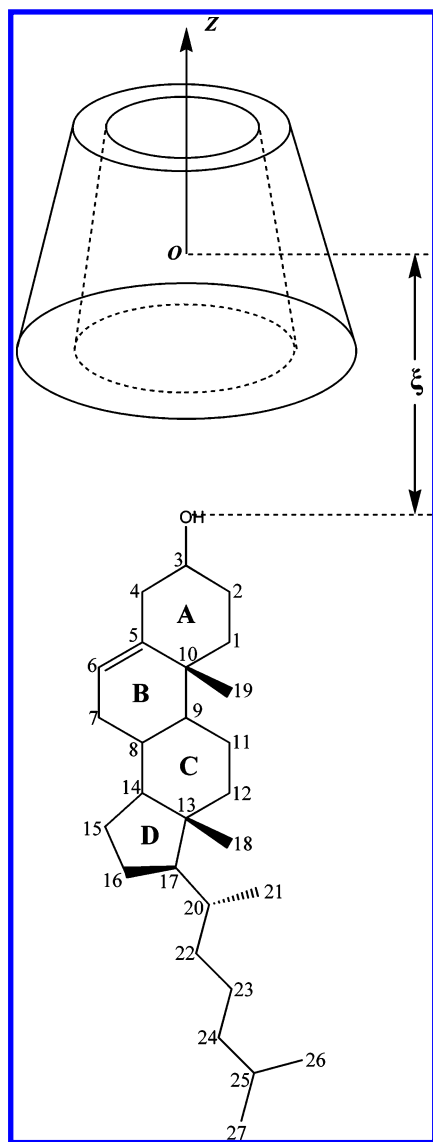


**Figure 1.** Schematic representation of the initial structure in which the carbon atoms of cholesterol are numbered and the four rings of cholesterol are labeled with capital letters.

## 2. Methods and Computational Details

**2.1. Molecular Models.** The initial coordinates of  $\beta$ -CD and DM- $\beta$ -CD were taken from three-dimensional crystal structures.<sup>35,36</sup> The coordinates of HP- $\beta$ -CD were obtained using insight II,<sup>37</sup> introducing six 2-hydroxypropyl groups in the 2 and 6 positions of  $\beta$ -CD. Last, the coordinates of cholesterol come from solid-state structure at room temperature.<sup>38</sup> The structures of the three CDs and cholesterol were energy-minimized using a conjugate gradient-like algorithm. Because translocation of the hydroxyl terminal region of cholesterol occurs through the narrow mouth of the CDs,<sup>23,27</sup> only the orientation of cholesterol facing the wide entrance of all three CDs was considered here. During the MD simulations, the glycosidic oxygen atoms of CDs were coerced to their initial position using a soft harmonic restraint to ensure that cholesterol remains included into the CD cavity from its wide entrance. Because  $\beta$ -CDs have a rather rigid skeleton and, hence, may be regarded as rigid bodies,<sup>39–41</sup> harmonic restraints should not affect the flexibility of CDs appreciably. Figure 1 provides a schematic representation of the initial structure in which the carbon atoms of cholesterol are numbered, and the four rings of cholesterol are labeled A, B, C, and D. CDs and cholesterol

are oriented with their principal axis aligned with the  $z$  axis. The center of mass of CD is set to the origin of the coordinate system, and the  $z$  axis points toward the primary side of CD. Cholesterol was introduced into the CD cavity from its wide mouth. For hydration of the model, a water box confined by a period boundary condition was added to the simulation system. The initial size of the water box is  $38.7 \times 38.4 \times 58.8 \text{ \AA}^3$  for  $\beta$ -CD,  $41.9 \times 42.5 \times 78.8 \text{ \AA}^3$  for HP- $\beta$ -CD, and  $41.4 \times 41.3 \times 68.8 \text{ \AA}^3$  for DM- $\beta$ -CD, involving 2618, 4278, and 3218 water molecules, respectively.

**2.2. Molecular Dynamics Simulations.** All MD simulations were performed using the program NAMD<sup>42</sup> with the CHARMM force field<sup>43</sup> and the TIP3P water model.<sup>44</sup> The topology of cholesterol is identical to that used in ref 45. The equations of motion were integrated with a 1-fs time step. The lengths of those covalent bonds between heavy and hydrogen atoms were frozen to their equilibrium value. The temperature was maintained at 298 K, employing Langevin dynamics with a damping coefficient of  $1 \text{ ps}^{-1}$ . The Nosé–Hoover Langevin piston was used to control the pressure at 1 atm, with a piston period of 100 fs, a damping time constant of 50 fs, and a piston temperature of 298 K. The van der Waals cutoff was set to 14  $\text{\AA}$ . Long-range electrostatic forces were taken into account by means of the particle-mesh Ewald approach. The present set of calculations was carried out on a HP Integrity rx2600 (Itanium2 based) Cluster with a Myrinet 2000 switch.

**2.3. Free Energy Calculations.** The free energy along an appropriate ordering parameter,  $\xi$ , describing host–guest association was estimated using the ABF method in which a biasing force is rapidly estimated and refined to erase the ruggedness of the free energy surface, and, hence, allow  $\xi$  to be sampled uniformly. Next, the free energy is determined by integrating the average force acting along  $\xi$ , obtained from unconstrained MD simulations.<sup>31–34</sup> Compared to other schemes in the spirit of the umbrella sampling method,<sup>46</sup> no initial guess of the bias is necessary, thereby improving the efficiency and reducing the cost of the calculations.<sup>32,33</sup> Prior to each ABF run, the molecular assemblies formed by the CDs, cholesterol, and their aqueous medium were equilibrated over a period of 500 ps. In the present ABF calculations, the ordering parameter was chosen as the distance separating a reference atom of cholesterol, viz. the oxygen atom of its hydroxyl moiety, from the center of mass of the CD backbone along the  $z$  direction of Cartesian space. For the three systems, convergence was probed by extending the total simulation time and assessing the evolution of the average force as a function of time. The pathway, viz.  $-10 \leq \xi \leq 22 \text{ \AA}$ , was divided into eight consecutive windows to further increase the efficiency of the calculations. Over 2 ns of sampling were generated in each window, irrespective of the host–guest complex. Instantaneous values of the force were accrued in bins 0.1  $\text{\AA}$  wide. One thousand samples were accumulated in each bin prior to application of the adaptive bias. The average force was interpolated over eight adjacent bins and progressively applied along  $\xi$  by means of a linear ramp. The standard error of the free energy difference was estimated using the expression given by Rodriguez-Gomez et al.<sup>34</sup>

## 3. Results and Discussion

**3.1. Free Energy Profile along the Ordering Parameter.** The free energy profiles characterizing inclusion of cholesterol into  $\beta$ -CD, HP- $\beta$ -CD, and DM- $\beta$ -CD are depicted, respectively, in Figure 2a–c. In the latter, it was chosen conventionally to set the free energy at zero for the maximal separation of CD

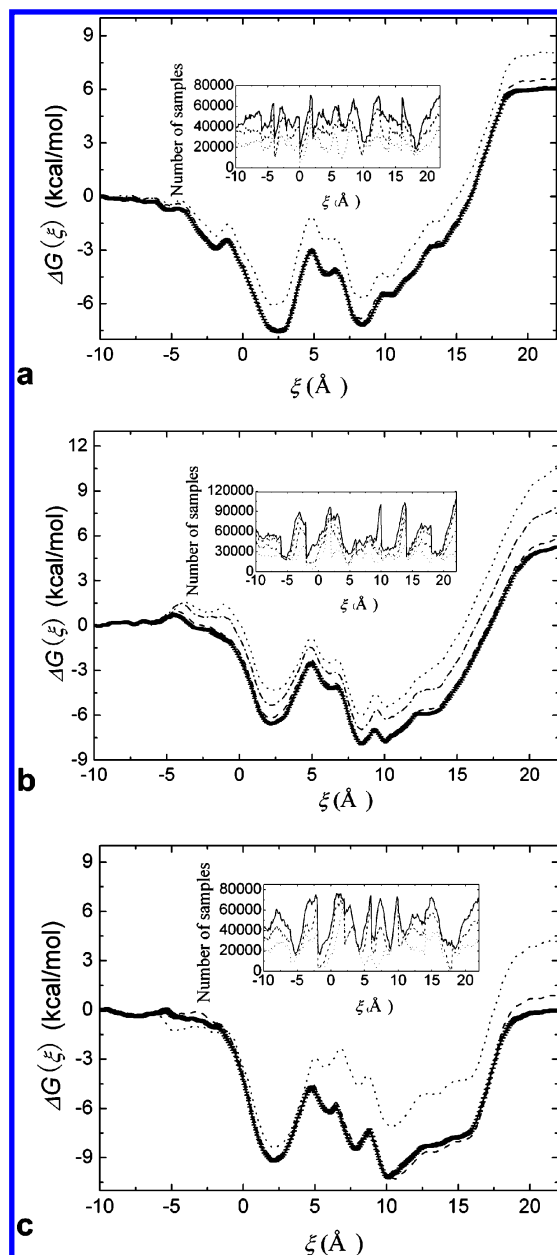


**Figure 2.** Free energy profile obtained from ABF calculation for the inclusion of cholesterol into CD. The sampling distribution characteristic of each MD simulation is included in the inset. The error bars in the figure represent the standard error of the free energy difference at each  $\xi$  in the final free energy profile. (a) The free energy profiles for the inclusion of cholesterol into  $\beta$ -CD, obtained from 8-ns (dotted line), 12-ns (dashed line), and 16-ns (solid line) simulations. (b) The free energy profiles for the inclusion of cholesterol into HP- $\beta$ -CD, obtained from 8-ns (dotted line), 12-ns (dashed dot line), 16-ns (dash line), and 18-ns (solid line) simulations. (c) The free energy profiles for the inclusion of cholesterol into DM- $\beta$ -CD, obtained from 8-ns (dotted line), 12-ns (dashed line), and 16-ns (solid line) simulations.

and cholesterol. From the onset, it can be seen that, qualitatively, these free energy profiles have a similar shape, with two local minima and a barrier separating them.

For the inclusion of cholesterol into  $\beta$ -CD (see Figure 2a), it would appear that 16 ns is sufficient to obtain a reasonably converged PMF. A closer look at Figure 2a reveals that the free energy decreases as cholesterol approaches  $\beta$ -CD, leading to the first minimum around 2.5 Å, with a free energy of ca. -7.5 kcal/mol. The structure of this stationary point is shown in Figure 3a. In this host-guest complex, the A and B rings of cholesterol are buried in the cavity of  $\beta$ -CD and the hydroxyl

group of cholesterol is located near the narrow side of  $\beta$ -CD cavity. As cholesterol penetrates deeper in the cavity of  $\beta$ -CD, an energy barrier of approximately 4 kcal/mol emerges at about 5 Å, arising from steric hindrances. This corresponds to the methyl group of cholesterol C10 crossing the narrow end of  $\beta$ -CD. The second minimum occurs around 8.4 Å with a free energy of -7.2 kcal/mol. In this second host-guest complex, shown in Figure 3b, the A ring of cholesterol and the C10 methyl group are outside the  $\beta$ -CD cavity. The C and D rings, and a portion of the B ring, are buried in the  $\beta$ -CD cavity. As cholesterol subsequently leaves the cavity of the CD, the free energy increases progressively, and eventually reaches a plateau when the two chemical species no longer interact.

Figure 2b shows the free energy profile delineating the inclusion of cholesterol into HP- $\beta$ -CD, based on different simulation times. The absence of noteworthy differences between the curves generated from 16- and 18-ns runs suggests that an 18-ns simulation may be sufficient to obtain a reasonable estimate of the free energy along the ordering parameter. Just like that for  $\beta$ -CD, the free energy landscape also features two minima and a barrier separating the latter. The approximately 4 kcal/mol-high free energy barrier is also located around 5 Å, resulting from steric hindrances. The two minima occur at ca. 2.2 and 8.5 Å, with a free energy of -6.6 and -7.9 kcal/mol, close to those characteristics of  $\beta$ -CD. These results tend to indicate that the positions of cholesterol in the cavity of  $\beta$ -CD and HP- $\beta$ -CD are very similar.

In the case of the inclusion of cholesterol into DM- $\beta$ -CD, convergence of the free energy seems to be reached after 16 ns. As shown in Figure 2c, the free energy landscape consists of two deeper minima occurring at 2.1 and 10.2 Å and corresponding to free energies of -9.2 and -10.2 kcal/mol, respectively. The free energy barrier separating the two minima is markedly broader than that of  $\beta$ -CD and HP- $\beta$ -CD. The structure of the stationary point around 2.1 Å is shown in Figure 3c. The A ring, B ring, and a portion of the C ring of cholesterol are inserted in the DM- $\beta$ -CD cavity. Introduction of methyl functional groups deepens the hydrophobic cavity of DM- $\beta$ -CD to such an extent that the hydroxyl moiety is still confined inside the latter. The structure of the complex near 10.2 Å is shown in Figure 3d. The methyl group causing steric hindrances has now left the hydrophobic cavity of DM- $\beta$ -CD. Moreover, portions of the B, C, and D rings as well as of the hydrocarbon tail are also embedded in the DM- $\beta$ -CD cavity, thereby resulting in favorable van der Waals contacts.

### 3.2. Association Constants and Association Free Energies.

The association constant may be obtained by integrating the PMF along the ordering parameter,  $\xi$ , to the limit of association of cholesterol and CD.<sup>48</sup> When cholesterol penetrates within the CD cavity, the trajectory is confined in a small cylinder and the sampled volume of configurational space is restrained to that cylinder, the cross section of which is defined by the possible ( $x$ ,  $y$ )-movement of cholesterol in the cavity. The 1 M-standardized association constant may, therefore, be written as

$$K_a = \pi N_A \int r_{ave}^2 \exp[-\Delta G(\xi)/RT] d\xi$$

where  $N_A$  is Avogadro's number and  $R$  is the ideal gas constant.  $r_{ave}$  is the average radius of the cross section in each bin, which evidently varies with  $\xi$ . The integration limit is the interval over which host-guest association is witnessed. The space integration over  $\xi < 0$  corresponds to the reference atom of cholesterol located by the wide entrance of CD, whereas for  $\xi > 0$ , this



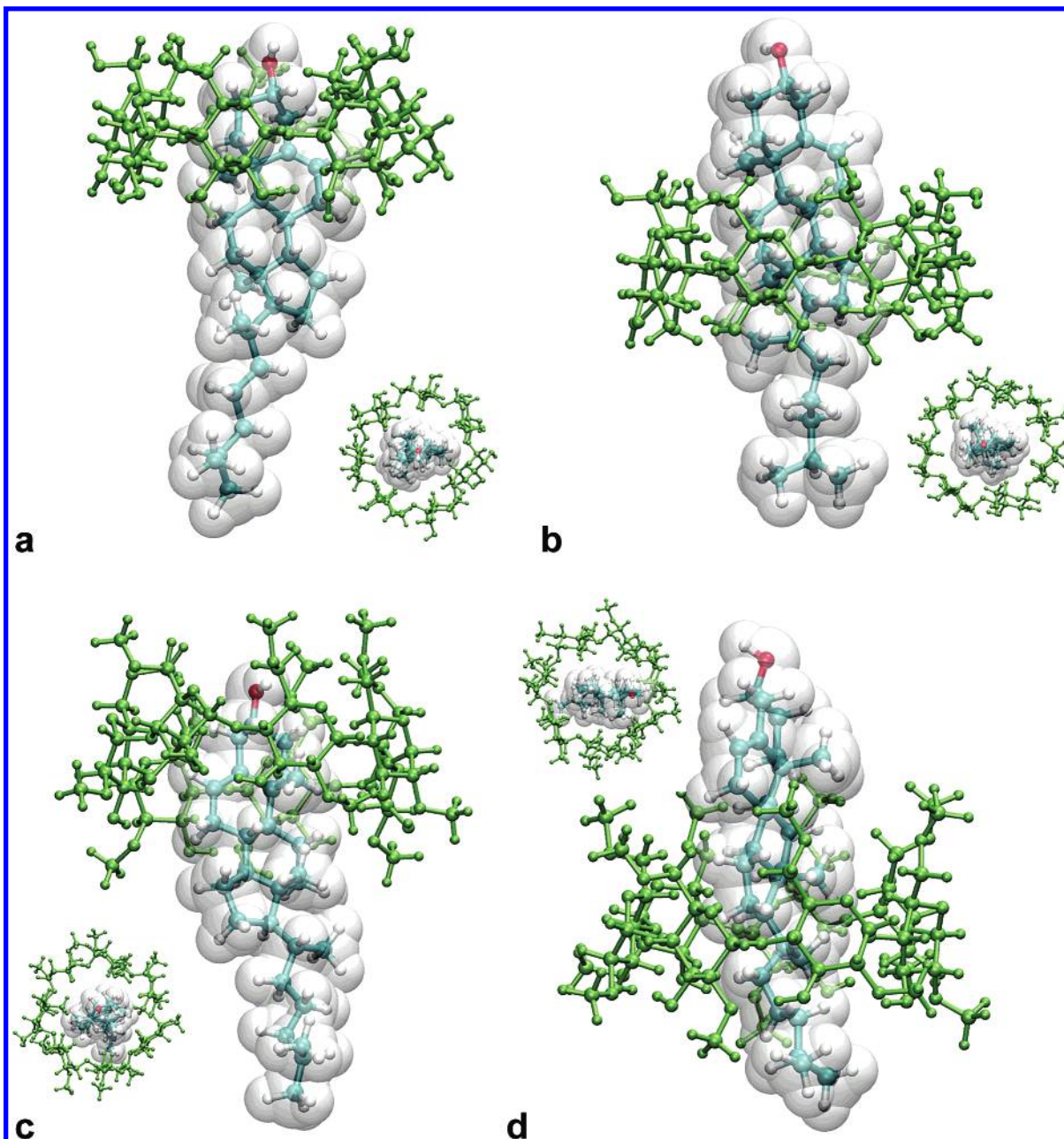


**Figure 3.** Snapshot of the host–guest complexes near the free energy minima: (a) inclusion of cholesterol into  $\beta$ -CD near the first minimum, i.e.,  $\xi = 2.5$  Å. (b) inclusion of cholesterol into  $\beta$ -CD near the second minimum, i.e.,  $\xi = 8.4$  Å. (c) inclusion of cholesterol into DM- $\beta$ -CD near the first minimum, i.e.,  $\xi = 2.1$  Å. (d) inclusion of cholesterol into DM- $\beta$ -CD near the second minimum, i.e.,  $\xi = 10.2$  Å. For clarity, water molecules are not shown. Inset: top view of the complexes. Image rendering was obtained with the VMD visualization program.<sup>47</sup>

atom is by the narrow entrance of CD. From the expression of  $K_a$ , the association free energy may be recovered through

$$\Delta G_{\text{bind}} = -RT \ln K_a$$

The computed association constants and association free energies are gathered in Table 1. These quantities reflect the ability of the CDs to bind cholesterol. From Table 1, the three CDs may be ranked according to their respective propensity to associate with cholesterol, namely, DM- $\beta$ -CD > HP- $\beta$ -CD >  $\beta$ -CD, which is consistent with experiment.<sup>7,8,11</sup> DM- $\beta$ -CD exhibits the strongest ability to bind cholesterol, a property likely to be related to its deeper hydrophobic cavity, compared to the two other  $\beta$ -CDs.

Interaction of cholesterol with CDs has been investigated amply at the experimental level in recent years. The stability

**TABLE 1: Association Constants and Association Free Energies of Cholesterol with  $\beta$ -Cd, HP- $\beta$ -CD, and DM- $\beta$ -CD**

host	$K_a^a$ (M <sup>-1</sup> )	$\Delta G_{\text{bind}}^a$ (kcal/mol)	$\Delta G_{\text{bind,exp}}^b$ (kcal/mol)
$\beta$ -CD	$1.9 \times 10^3$	−4.5	−5.7 <sup>c</sup>
HP- $\beta$ -CD	$1.8 \times 10^4$	−5.8	−5.8 <sup>c</sup>
DM- $\beta$ -CD	$5.5 \times 10^5$	−7.8	−2.8 (1:1) <sup>d</sup> −6.5 (1:2)

<sup>a</sup>  $K_a$  and  $\Delta G_{\text{bind}}$  are the calculated association constant and the association free energy, respectively. <sup>b</sup>  $\Delta G_{\text{bind,exp}}$  denotes the experimental result. <sup>c</sup> From ref 29. <sup>d</sup> From ref 27.

constants of the complexes formed by cholesterol and  $\beta$ -CD or HP- $\beta$ -CD were measured using spectral displacement techniques, resulting in association free energy values of −5.7 and −5.8 kcal/mol, respectively.<sup>29</sup> Nishijo et al. also measured the stability constants of cholesterol bound to several CDs using

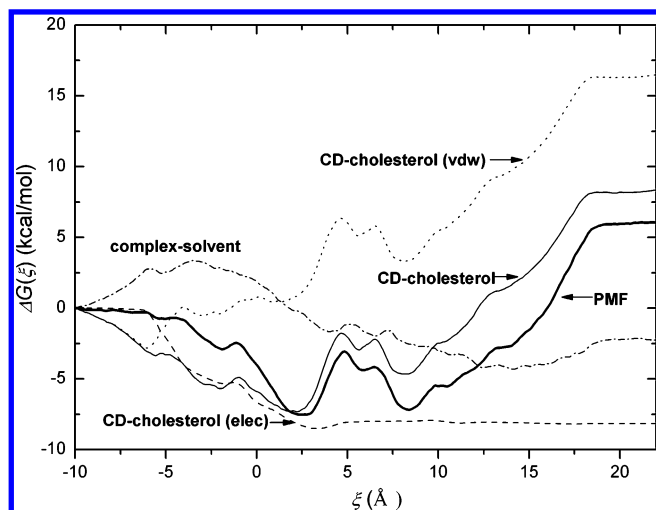


**Figure 4.** Partitioning of the PMF (thick solid line) into CD-cholesterol van der Waals (dotted line), CD-cholesterol electrostatic (dashed line), and complex-solvent contributions (dashed-dotted line) for the inclusion of cholesterol into  $\beta$ -CD. CD-cholesterol (solid line) is the sum of CD-cholesterol van der Waals and electrostatic contributions.

solubility methods.<sup>26,27</sup> No complex was detected for cholesterol and  $\beta$ -CD, and only a marginally soluble complex was detected in the case of cholesterol binding HP- $\beta$ -CD. DM- $\beta$ -CD was assumed to form two types of complexes with molar ratios of 1:1 and 1:2, corresponding, respectively, to association free energies of -2.8 and -6.5 kcal/mol.

Comparison of computationally and experimentally determined association constants is by and large a cumbersome task because the latter may depend strongly on the experimental method chosen.<sup>3,49</sup> Association constants measured by experimental methods reflect the stability of the complex, which is necessarily affected by the experimental conditions, for example, temperature and pH. In experiments, the CDs investigated here may form 2:1 or 3:1 complexes with cholesterol. Moreover, the association constants for the complex of CDs and organic molecules measured employing alternative methods are found to vary over several orders of magnitude.<sup>3,49</sup> From a theoretical

perspective, sources of errors, beyond the appropriateness of the potential energy function, are likely to be rooted in the incomplete sampling of the configurational space imposed by the choice of the ordering parameter,  $\xi$ , guiding host-guest association. How this choice modulates the estimated free energy differences is yet unclear, and a precise quantification of such an effect is outside the scope of the present contribution.

**3.3. Driving Force Responsible for Association.** The driving force responsible for holding the host-guest complex together constitutes a crucial issue in CD inclusion studies. To address this point, we calculated the free energy contributions by partitioning the total force acting along  $\xi$  into two main terms, viz. the CD-cholesterol and the complex-solvent terms, and integrating these force contributions separately.

The different contributions to the free energy along  $\xi$  for the inclusion of cholesterol into  $\beta$ -CD are shown in Figure 4. From ca. -4.0 Å to the first minimum about 2.5 Å, the CD-cholesterol van der Waals contribution is nearly constant. Entering of cholesterol into the  $\beta$ -CD cavity is driven mainly by the CD-cholesterol electrostatic contribution. As cholesterol penetrates deeper in the cavity of  $\beta$ -CD to form the inclusion complex, the electrostatic term remains roughly constant between 2.5 and 8.4 Å. The change in free energy arises mainly from that of CD-cholesterol van der Waals and complex-solvent contributions. This suggests that the association of cholesterol with  $\beta$ -CD in this interval is essentially driven by van der Waals interactions and solvation effects. The free energy barrier of the total PMF results principally from an increase of the CD-cholesterol van der Waals contribution. For the inclusion of cholesterol into HP- $\beta$ -CD and DM- $\beta$ -CD, the contributions to the total free energy exhibit very similar characteristics.

**3.4. Structural Stability of the Complex.** The structural stability of the complex is yet another critical aspect of CD inclusion studies. To gain further insight into this issue, we performed additional MD simulations over 5 ns using the complex structure near the free energy minima as a starting point.

Figure 5a shows the variations of  $\xi$  and the interaction energy between the host and the guest in the complex of  $\beta$ -CD with

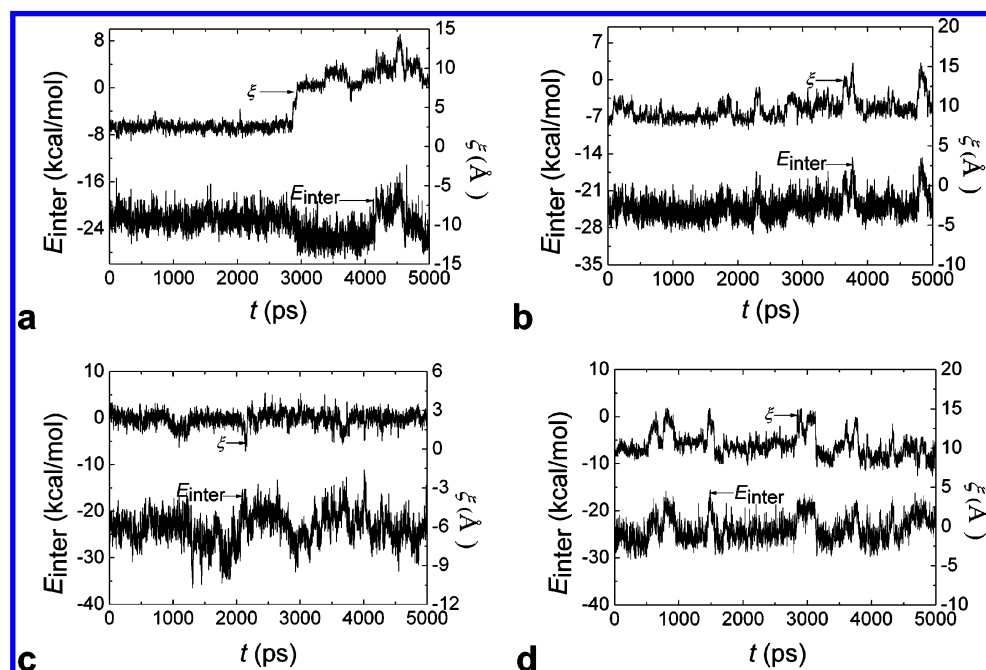


**Figure 5.** Variations of  $\xi$  and the interaction energy obtained from an additional 5-ns MD simulation, using the host-guest complex structures of Figure 3a (a), Figure 3b (b), Figure 3c (c), and Figure 3d (d).

cholesterol near 2.5 Å. From this profile, it may be observed that the interaction energy decreases and  $\xi$  increases abruptly beyond 3 ns. This change can be ascribed to modifications in the structure of the complex (see Figure 3a and b). It may be further inferred that the structure of the complex in Figure 3a is stable. Evolution of the complex to the structure of Figure 3b is possible, albeit difficult. During the MD simulation, significant fluctuation of the energy can be seen around 4.2 ns. This corresponds to the less stable structure of the complex involving only the hydrocarbon chain inserted into the  $\beta$ -CD cavity. A distinct 5-ns MD simulation was carried out for the complex of  $\beta$ -CD with cholesterol at the second minimum, at ca. 8.4 Å. Variations of  $\xi$  and the interaction energy are shown in Figure 5b. No abrupt variation of these quantities is detected. This indicates that the complex structure is appreciably stable over the length of the MD simulation. We note in passing that the trajectory of the complex of HP- $\beta$ -CD is very similar to that of  $\beta$ -CD (data not shown here).

Last, Figure 5c shows the variations of  $\xi$  and the interaction energy between host and guest for the complex of DM- $\beta$ -CD with cholesterol at the first minimum, ca. 2.2 Å. While the interaction energy fluctuates,  $\xi$  remains roughly constant. This result suggests that the structure of the complex is very stable, and no structural transition is to be found over the MD simulation. To verify whether 5 ns of sampling is sufficient to observe the stability of the system in the local minimum, we carried out a longer time, 10 ns, MD simulation. The results from the 5-ns and 10-ns simulations are shown to coincide nicely. It is possible that the broader energy barrier (see Figure 2c) hinders such transition, viz. transition from the structure of Figure 3c to that of Figure 3d. Formation of the inclusion complex depicted in Figure 3d is difficult because of the larger free energy barrier compared to  $\beta$ -CD and HP- $\beta$ -CD. Figure 5d shows the variations of both  $\xi$  and the interaction energy for the complex of DM- $\beta$ -CD with cholesterol at the second minimum, viz. 10.2 Å. Just like in Figure 5b, no significant fluctuation occurs during the simulation, suggesting that the complex of Figure 3d is equally stable, at least over the time scale explored herein.

Additional 5-ns MD simulations were also performed, using as a starting point a structure of the complex that does not correspond to a local minimum of the free energy hyperplane but that is located between its first and second minimum. For example, in the case of  $\beta$ -CD, the MD simulation was performed using as a starting point the complex at about 4.1 Å, obtained randomly between the first minimum (ca. 2.5 Å) and the peak of the free energy barrier (ca. 5 Å). Analyzing the MD trajectories, our results coincide remarkably with those obtained for the first minimum (as in Figure 5a). In the first 1.7 ns, sampling of  $\xi$  remained focused near the first minimum, viz. 2.5 Å. A structural transition was then observed, causing  $\xi$  to be sampled preferentially near the second minimum, viz. 8.4 Å. An extra MD simulation starting from the point chosen randomly between the peak of the free energy barrier, viz. 5 Å, and the second minimum, viz. 8.4 Å, was also carried out. In the latter, sampling of  $\xi$  essentially fluctuates near the second minimum. A similar behavior may be witnessed in the case of HP- $\beta$ -CD. For DM- $\beta$ -CD, however, the choice of distinct starting points affects the results only marginally, on account of a rapid equilibration toward the first or second local minimum.

#### 4. Conclusions

The free energy profiles characterizing the inclusion of cholesterol into  $\beta$ -CD, HP- $\beta$ -CD, and DM- $\beta$ -CD were deter-

mined using the recent, cost-effective ABF approach. The present set of results reveals the existence of two preferred binding modes along the reaction pathway. Comparison of the calculated association constants and association free energies highlights the highest propensity of DM- $\beta$ -CD to bind cholesterol, and, hence, its anticipated ability to extract the latter for lipid bilayers.<sup>7,8,11,30</sup> Furthermore, from the free energy calculations reported herein, a ranking for cholesterol binding affinity may be proposed, viz. DM- $\beta$ -CD > HP- $\beta$ -CD >  $\beta$ -CD, which is in line with experiment.<sup>7,8,11</sup> Partitioning of the PMF into free energy contributions illuminates how the nature of the driving force for host-guest inclusion changes at the different stages of the process. Last, additional MD simulations targeted at probing the intrinsic stability of the complexes at the free energy minima suggest that, unlike for  $\beta$ -CD and HP- $\beta$ -CD, only one complex is preferred kinetically for DM- $\beta$ -CD.

**Acknowledgment.** This study is supported by the Natural Science Foundation of China (nos. 20172048 and 20325517) and the Teaching and Research Award Program for Outstanding Young Professors (TRAPOYP) in Higher Education Institute, MOE, PRC. Thanks to USTC-HP High Performance Computing Joint Lab (HPCJL) for affording HP-cluster.

#### References and Notes

- (1) Simons, K.; Ikonen, E. *Science* **2000**, *290*, 1721–1726.
- (2) Szejtli, J. *Chem. Rev.* **1998**, *98*, 173–1753.
- (3) Rekharsky, M. V.; Inoue, Y. *Chem. Rev.* **1998**, *98*, 1875–1917.
- (4) Cai, W. S.; Yu, Y. M.; Shao, X. G. *J. Mol. Model.* **2005**, *11*, 186–193.
- (5) Cai, W. S.; Yao, X. X.; Shao, X. G.; Pan, Z. X. *J. Inclusion Phenom. Macrocyclic Chem.* **2005**, *51*, 41–51.
- (6) Cai, W. S.; Yu, Y. M.; Shao, X. G. *Chemom. Intell. Lab. Syst.*, in press.
- (7) Visconti, P. E.; Galantino-Homer, H.; Ning, X. P.; Moore, G. D.; Valenzuela, J. P.; Jorgez, C. J.; Alvarez, J. G.; Kopf, G. S. *J. Biol. Chem.* **1999**, *274*, 3235–3242.
- (8) Kilsdonk, E. P.; Yancey, P. G.; Stoudt, G. W.; Bangerter, F. W.; Johnson, W. J.; Phillips, M. C.; Rothblat, G. H. *J. Biol. Chem.* **1995**, *270*, 17250–17256.
- (9) Klein, U.; Gimpl, G.; Fahrenholz, F. *Biochemistry* **1995**, *34*, 13784–13793.
- (10) Debouzy, J. C.; Fauvel, F.; Crouzy, S.; Girault, L.; Chapron, Y.; Goschl, M.; Gabelle, A. *J. Pharm. Sci.* **1998**, *87*, 59–66.
- (11) Yancey, P. G.; Rodriguez, W. V.; Kilsdonk, E. P. C.; Stoudt, G. W.; Johnson, W. J.; Phillips, M. C.; Rothblat, G. H. *J. Biol. Chem.* **1996**, *271*, 16026–16034.
- (12) Ohvo, H.; Olsio, C.; Slotte, J. P. *Biochim. Biophys. Acta* **1997**, *1349*, 131–141.
- (13) Rajewskix, R. A.; Stella, V. J. *J. Pharm. Sci.* **1996**, *85*, 1142–1169.
- (14) Irie, T.; Uekama, K. *J. Pharm. Sci.* **1997**, *86*, 147–162.
- (15) Pitha, J.; Irie, T.; Sklar, P. B.; Nye, J. S. *Life Sci.* **1988**, *43*, 493–502.
- (16) Christian, A. E.; Byun, H. S.; Zhong, N.; Wanunu, M.; Marti, T.; Furer, A.; Diederich, F.; Bittman, R.; Rothblat, G. H. *J. Lipid Res.* **1999**, *40*, 1475–1482.
- (17) Irie, T.; Fukunaga, K.; Pitha, J. *J. Pharm. Sci.* **1992**, *81*, 521–523.
- (18) Atger, V. M.; Moya, M. D.; Stoudt, G. W.; Rodriguez, W. V.; Phillips, M. C.; Rothblat, G. H. *J. Clin. Invest.* **1997**, *99*, 773–780.
- (19) Haynes, M. P.; Phillips, M. C.; Rothblat, G. H. *Biochemistry* **2000**, *39*, 4508–4517.
- (20) Ohvo, H.; Slotte, J. P. *Biochemistry* **1996**, *35*, 8018–8024.
- (21) Radhakrishnan, A.; McConnell, H. M. *Biochemistry* **2000**, *39*, 8119–8124.
- (22) Niu, S. L.; Litman, B. J. *Biophys. J.* **2002**, *83*, 3408–3415.
- (23) Ravichandran, R.; Divakar, S. *J. Inclusion Phenom. Macrocyclic Chem.* **1998**, *30*, 253–270.
- (24) Podar, K.; Tai, Y. T.; Cole, C. E.; Hideshima, T.; Sattler, M.; Hamblin, A.; Mitsiades, N.; Schlossman, R. L.; Davies, F. E.; Morgan, G. J.; Munshi, N. C.; Chauhan, D.; Anderson, K. C. *J. Biol. Chem.* **2003**, *278*, 5794–5801.
- (25) Choi, Y. H.; Yang, C. H.; Kim, H. W.; Jung, S. *J. Inclusion Phenom. Macrocyclic Chem.* **2001**, *39*, 71–76.
- (26) Nishijo, J.; Moriyama, S.; Shiota, S.; Kamigauchi, M.; Sugiura, M. *Chem. Pharm. Bull.* **2004**, *52*, 1405–1410.



- (27) Nishijo, J.; Moriyama, S.; Shiota, S. *Chem. Pharm. Bull.* **2003**, *51*, 1253–1257.
- (28) Breslow, R.; Zhang, B. L. *J. Am. Chem. Soc.* **1996**, *118*, 8495–8496.
- (29) Frijlink, H. W.; Eissens, A. C.; Hefting, N. R.; Poelstra, K.; Lerk, C. F.; Meijer, D. K. F. *Pharm. Res.* **1991**, *8*, 9–16.
- (30) Rodal, S. K.; Skretting, G.; Garred, O.; Vilhardt, F.; van Deurs, B.; Sandvig, K. *Mol. Biol. Cell* **1999**, *10*, 961–974.
- (31) Darve, E.; Pohorille, A. *J. Chem. Phys.* **2001**, *115*, 9169–9183.
- (32) Hénin, J.; Pohorille, A.; Chipot, C. *J. Am. Chem. Soc.* **2005**, *127*, 8478–8484.
- (33) Hénin, J.; Chipot, C. *J. Chem. Phys.* **2004**, *121*, 2904–2914.
- (34) Rodriguez-Gomez, D.; Darve, E.; Pohorille, A. *J. Chem. Phys.* **2004**, *120*, 3563–3570.
- (35) Betzel, C.; Saenger, W.; Hingerty, B. E.; Brown, G. M. *J. Am. Chem. Soc.* **1984**, *106*, 7545–7557.
- (36) Aree, T.; Saenger, W.; Leibnitz, P.; Hoier, H. *Carbohydr. Res.* **1999**, *315*, 199–205.
- (37) *Insight II User Guide*; Accelrys Software Inc.: San Diego, CA, 2005.
- (38) Shieh, H. S.; Hoard, L. G.; Nordman, C. E. *Acta Crystallogr.* **1981**, *B37*, 1538–1543.
- (39) Saenger, W. R.; Jacob, J.; Gessler, K.; Steiner, T.; Hoffmann, D.; Sanbe, H.; Koizumi, K.; Smith, S. M.; Takaha, T. *Chem. Rev.* **1998**, *98*, 1787–1802.
- (40) Schneider, H. J.; Hacket, F.; Rudiger, V.; Ikeda, H. *Chem. Rev.* **1998**, *98*, 1755–1785.
- (41) Hamelin, B.; Jullien, L.; Laschewsky, A.; du Penhoat, C. H. *Chem.—Eur. J.* **1999**, *5*, 546–556.
- (42) Phillips, J. C.; Braun, R.; Wang, W.; Gumbart, J.; Tajkhorshid, E.; Villa, E.; Chipot, C.; Skeel, R. D.; Kalé, L.; Schulten, K. *J. Comput. Chem.* **2005**, *26*, 1781–1802.
- (43) MacKerell, A. D., Jr.; Bashford, D.; Bellott, R. L.; Dunbrack, R. L., Jr.; Evanseck, J. D.; Field, M. J.; Fischer, S.; Gao, J.; Guo, H.; Ha, S.; Joseph-McCarthy, D.; Kuchnir, L.; Kuczera, K.; Lau, F. T. K.; Mattos, C.; Michnick, S.; Ngo, T.; Nguyen, D. T.; Prodhom, B.; Reiher, W. E., III.; Roux, B.; Schlenkrich, M.; Smith, J. C.; Stote, R.; Straub, J.; Watanabe, M.; Wiorkiewicz-Kuczera, J.; Yin, D.; Karplus, M. *J. Phys. Chem. B* **1998**, *102*, 3586–3616.
- (44) Jorgensen, W. L.; Chandrasekhar, J.; Madura, J. D.; Impey, R. W.; Klein, M. L. *J. Chem. Phys.* **1983**, *79*, 926–935.
- (45) Pitman, M. C.; Suits, F.; MacKerell, A. D., Jr.; Feller, S. E. *Biochemistry* **2004**, *43*, 15318–15328.
- (46) Torrie, G. M.; Valleau, J. P. *J. Comput. Phys.* **1977**, *23*, 187–199.
- (47) Humphrey, W.; Dalke, A.; Schulten, K. *J. Mol. Graphics* **1996**, *14*, 33–38.
- (48) Shoup, D.; Szabo, A. *Biophys. J.* **1982**, *40*, 33–39.
- (49) Mwakibete, H.; Cristantino, R.; Bloor, D. M.; Wyn-Jones, E.; Holzwarth, J. F. *Langmuir* **1995**, *11*, 57–60.